Non-Linear Matters: Auxetic Surfaces

Olga Mesa
MaP+S Group Harvard University
Roger Williams University

Milena Stavric
Graz University of Technology

Saurabh Mhatre
MaP+S Group Harvard University

Jonathan Grinham
MaP+S Group Harvard University

Sarah Norman
MaP+S Group Harvard University

Allen Sayegh
MaP+S Group Harvard University

Martin Bechthold
MaP+S Group Harvard University

1

ABSTRACT

Auxetic structures exhibiting non-linear buckling are a prevalent research topic in the material sciences due to the ability to tune their reversible actuation, porosity, and negative Poisson's ratio. However, the research is limited to feature sizes at scales below 10 mm^2, and to date, there are no available efficient design and prototyping methods for architectural designers. Our study develops design principles and workflow methods to transform standard materials into auxetic surfaces at an architectural scale. The auxetic behavior is accomplished through buckling and hinging by subtracting from a homogeneous material to create perforated patterns. The form of the perforations, including shape, scale, and spacing, determines the behavior of multiple compliant "hinges" generating novel patterns that include scaling and tweening transformations. An analytical method was introduced to generate hinge designs in four-fold symmetric structures that approximate non-linear buckling. The digital workflow integrates a parametric geometry model with non-linear finite element analysis (FEA) and physical prototypes to rapidly and accurately design and fabricate auxetic materials. A robotic 6-axis waterjet allowed for rapid production while maintaining needed tolerances. Fabrication methods allowed for spatially complex shaping, thus broadening the design scope of transformative auxetic material systems by including graphical and topographical biases. The work culminated in a large-scale fully actuated and digitally controlled installation. It was comprised of auxetic surfaces that displayed different degrees of porosity, contracting and expanding while actuated electromechanically. The results provide a promising application for the rapid design of non-linear auxetic materials at scales complimentary to architectural products.

1 Experimental installation featuring auxetic surface modules electromechanically actuated.

INTRODUCTION

Over the past decade, interest in buildings that are able to adapt to human and environmental inputs via kinetically configurable systems such as facades has steadily grown. However, built examples often suffer from the need for complex mechanisms that are failure prone, expensive, and difficult to design and maintain. In this context the paper presents an alternative to the mechanical paradigm—computational and prototypical studies that utilize patterned elastic metamaterials that transform kinetically due to buckling and hinging deformations. A particular focus of the study are auxetic systems that exhibit negative Poisson's ratio behavior. These auxetic surfaces, a subset of metamaterials, feature significant transformations in overall size and in porosity.

Existing research on auxetic materials has generally focused on understanding geometrical design and computational methods that were prototyped on a small scale, with samples in the order of 200 mm side length. Our research focuses on architectural-scale applications. The study presents new design parameters for auxetic architectural systems, and develops and tests scale-appropriate rapid and precise digital production and prototyping methods. The novel design principles for architectural auxetic surfaces include scaling, tweening, and combinations of both transformations. These principles extend the design scope for auxetic architectural applications. Regular perforation patterns, which are well understood, can now be enhanced by non-standard patterns for novel aesthetic and performative effects. Research methods by the interdisciplinary team of designers, material scientists, and engineers include computational parametric studies of adaptive geometries, non-linear finite element analysis (FEA), and physical prototyping. The design and prototyping knowledge was tested in the design and digital production of an architecturally sized responsive ceiling system that deploys electromechanical actuation driven through a tablet interface (Figure 1).

BACKGROUND

Mechanical metamaterials are artificial materials exhibiting characteristics defined by geometry and structure rather than composition, with applications that include synthetic auxetics (Walser 2001; Kshetrimayum 2004; Lee et al. 2012). Poisson's ratio defines how a material expands (or contracts) transversely when being compressed (or stretched) longitudinally (Greaves et al. 2011). While most natural materials and typical elastic solids have a positive Poisson's ratio (in compression, the material conversely expands in the orthogonal direction), auxetic materials can exhibit negative Poisson's ratios. They can be found in nature, fabricated, or synthesized, and their behavior is independent of scale (Evans and Alderson 2000). The first known instance of a synthetic auxetic material was a foam with cells that unfolded when stretched (Lakes 1987). Given that this area is relatively new, much auxetic research has focused on discovery and documentation. Seeing no known approach to identify auxetic structures, researchers developed a system to do so utilizing Eigenmode analysis (Körner and Liebold-Ribeiro 2015). Another group studied behavior in auxetic cellular metamaterials across scales, finding key re-entrant and chiral auxetic 2D geometries and their respective features (Saxena et al. 2016). Others recently investigated known auxetic structures through a comparative study of 2D and 3D geometries, developing a CAD library to simulate behavior (Álvarez Elipe et al. 2012).

The Bertoldi group at Harvard have developed non-linear FEA methods that allowed the reliable, predictable design of novel auxetic patterns for transformable material systems in sheet form or as volume configurations. The pattern under investigation by the group features small, cell-like openings shaped such that buckling of the cell walls and subsequent hinging results in an overall auxetic behavior. Recent papers include explorations of pattern transformations and super-elastic behavior (Bertoldi et al. 2008), the relationship of pore shape on compaction through buckling (Overvelde, Shan, and Bertoldi 2012), and the relationship of pore shape to the non-linear response (Overvelde and Bertoldi 2014) in periodic elastomeric structures. Through these, it was found that mechanics of deformation can trigger dramatic pattern transformations (Bertoldi et al. 2008); that taking advantage of mechanical instabilities in soft/porous structures can lead to fast, reversible actuation applicable across scales (Overvelde, Shan, and Bertoldi 2012); and that pore shape strongly affects structural stability (Overvelde and Bertoldi 2014). Primarily investigating the behavior of identical cell geometries within a larger surface, none of the Bertoldi studies researched non-uniform patterns that involve scaling of cell size, changing the spacing of cells, or tweening of multiple cell geometries within a single larger surface. All of these elements are relevant for architectural applications where non-uniformity of cell patterns might be desired for visual or performative reasons.

Another group explored honeycomb patterns featuring a series of hinged planar surfaces that could be manufactured with additive or laminated-adhesive processes much like conventional honeycomb cores for sandwich panels. They also studied transitions between base-cell geometries, utilizing algorithmic curve attractors for gradual morphing transitions (Park et. al. 2015). However, this research did not investigate tweening and scaling transitions. These and other metamaterial prototypes have historically been limited to studies on the small product scale, where feature sizes are in the order of 5–30 mm. Examples of metamaterials, auxetics and cellular structures that have "scaled up," include a digital morphing wing (Jenett et al. 2016), nuclear core reactors

(Evans et al. 2000), deployable antennas for aerospace (Jacobs et al. 2012), and cellular sandwich panels for structural applications (Yang et al. 2013). None of these studies were developed at the architectural scale.

Although our case study utilized an external electromechanical actuator for large-scale modules, future actuation research could explore integrating actuation directly into the foam, potentially creating an auxetic structure at the molecular level (Álvarez Elipe et al. 2012). Current actuated examples include shape-memory materials, alloys, and polyurethane foams (Ivens et al. 2010), and layered, porous metamaterials capable of phase transformation due to changes in atmospheric pressure (rather than from an applied mechanical compression), creating a structure that also exhibits shape-memory behavior (Yang et al. 2016). Design of environmentally responsive metamaterials and auxetics is fundamental to the development of next-generation actuators, sensors, and smart-responsive surfaces (Babaee et al. 2013), potentially expanding actuated auxetic research at the architectural scale.

FUNDAMENTAL PRINCIPLES: PARAMETRIC ANALYSIS AND MATERIALITY

The main variables determining the behavior of auxetic systems include the geometric arrangement of the perforations and their geometry, including orientation, size, and ratio between solid and void. The use of parametric models facilitates the study of various systems and their resultant kinematic and material behaviors.

Symmetry and Nomenclature of Cell Perforations

To study the underlying geometric principles in metamaterial auxetic systems, we investigated the geometry belonging to the four-fold symmetry group p4m (Figure 2b). For the purposes of the study, we will refer to the area of the perforation and its corresponding solid portions as a quadrant, with point D at its center point (Figure 2a). The arbitrary profile curve p defines the boundary between solid and void (Figure 2a). The geometry of the quadrant can be divided into eight units, showing symmetries in four distinct directions: horizontal (h), vertical (v) and two diagonals (d1, d2) (Figure 2b). We will refer to the ⅛ of a quadrant and its corresponding portion of profile curve p as a unit (Figure 2c), and the ¼ of the quadrant and its corresponding portion of profile curve p as a cell (Figure 2d). The profile curve passing through the points A and B will be defined as curve m. Points A and B on the profile curve m mark the nearest position to the cell-bounding box. Reflecting a curve profile m/2 along its horizontal and vertical axis generates a pattern p4m, defining a complete perforation, called p (Figure 2a).

Kinematic System of Periodic Configuration

A kinematic system can be created by aggregating four quadrants and defining their common points as the points of rotation within an auxetic surface. Figure 3a shows a kinematic system k in the initial position, where four quadrants (q0, q1, q2, and q3) are connected by their common points. For now the material thickness at these points is zero—an assumption that will be discussed later on. Taking into account the four-fold symmetry, we define four points of rotation: A0=A3, A1=A2, B0=B1, B2=B3 (Figure 3a). The rotation results when external compression forces act on the boundary of the system (Figure 12). The initial response of the auxetic system is geometric instability, followed by buckling and hinging (Figure 3). Alternatively, rotation can be imparted by generating internal bending moments in the system. Point A0=A3 is the common point of quadrants q0 and q3, B0=B1 the common point of q0 and q1, A1=A2 the common point of q1 and q2, and B2=B3 the common point of q2 and q3. The boundary of the quadrants establishes a grid. By rotating the core quadrant q0 in a clockwise direction around activation point A0=A3, point B0=B1 will also rotate in the same direction. As all quadrants are connected with their common points, the entirely kinematic system k will be automatically actuated (Figures 3b and 3c).

Rotation of Cells and Porosity of Auxetic Surface

Figure 4a, 4b, and 4c show selected stages of the system k, displaying rotational angles, and thus a different arrangement of voids. Figures 4a and 4b present the same system as Figure 3, but with the rotation around point A in a counterclockwise direction. When comparing the systems shown in Figure 3c and Figure 4b, we conclude that the same profile curve causes two different configurations of voids. The core void is elongated along the vertical axis when rotating clockwise, and elongated along the horizontal axis when rotating counterclockwise.

Maximum Angle of Cell Rotation

The maximum angle of rotation is the angle defined between the vertical axis and the tangent line onto curve m through point A (Figure 4a). The profile curve m, with its peak point P, will be the limit for the solid portions of the cell when they encounter each other. Figure 4d shows arbitrary profile curves m with corresponding tangents from point A and maximum angles of rotation per the given profile curve. The porosity is directly related to the curve profile m. A straight curve profile m, between point A and point B, will result in a square perforation (Figure 5a). The angle of rotation ranging between -pi/4 to +pi/4, constitutes the maximum rotational angle (Figure 5b). Figures 5a, 5c, and 5d show a different activation of the kinematic system in relation to the activating point A.

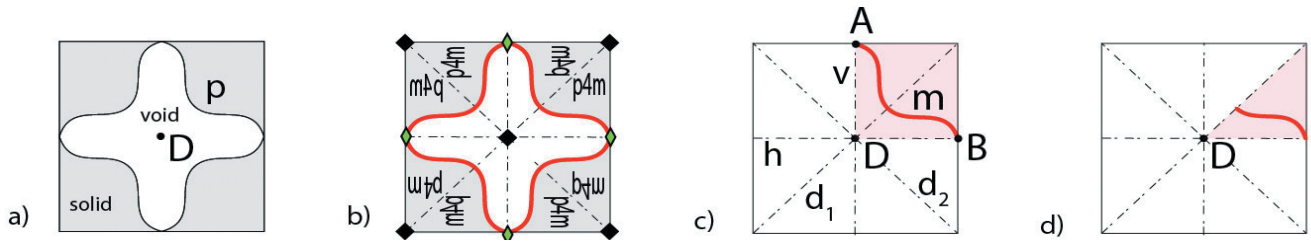

2

2 a) Quadrant with profile curve p – perforation, b) pattern p4m with rotation centers (90°, 180°), glide reflections and reflections, c) Cell and m as part of the profile curve, d) smallest possible part of pattern p4m-cell called Unit.

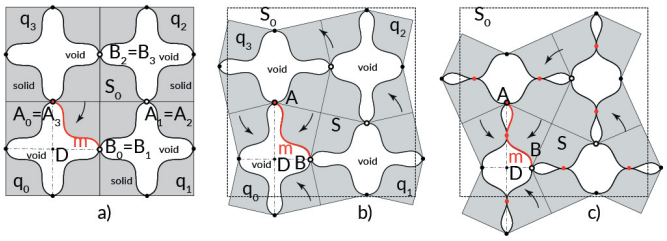

3

3 a) Kinematic system k in a base position with maximum area S0, b) activation of the system k in clockwise direction, c) maximum activation of the system k and changes of the base surface area S0 in shape and area.

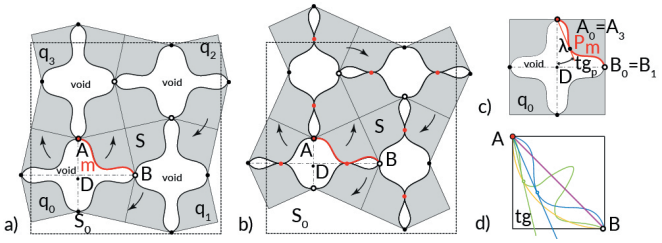

4

4 a) Rotation in counterclockwise direction, b) maximum activation causes minimal sizes of voids, c) the maximum rotation is defined by the geometry of profile curve and the angle between vertical axis and the tangent line onto curve m, d) different profile curves with corresponding tangents.

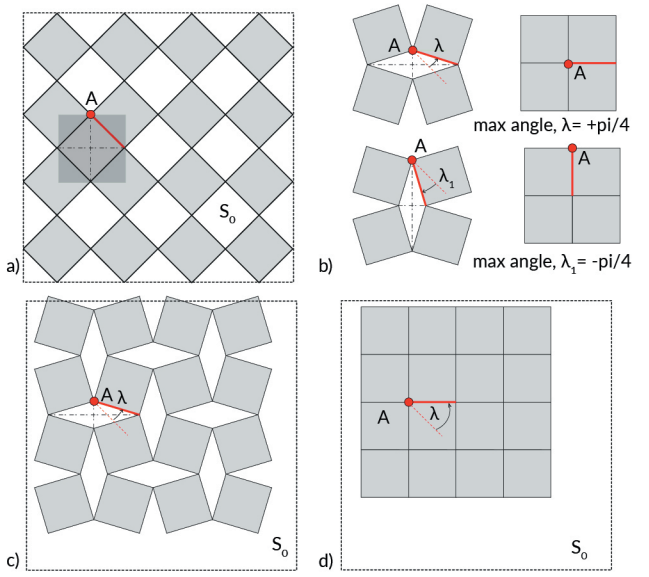

5

5 a) Profile curve m is a straight line and the system k is activating at point A, b) two different rotations, –λ and +λ, and new position related to the original quadrant marked in dark gray c) one of the activation positions in clockwise direction, solid: void 1:0.5 d) maximum activation λ= pi/4, solid: void = 1:0.

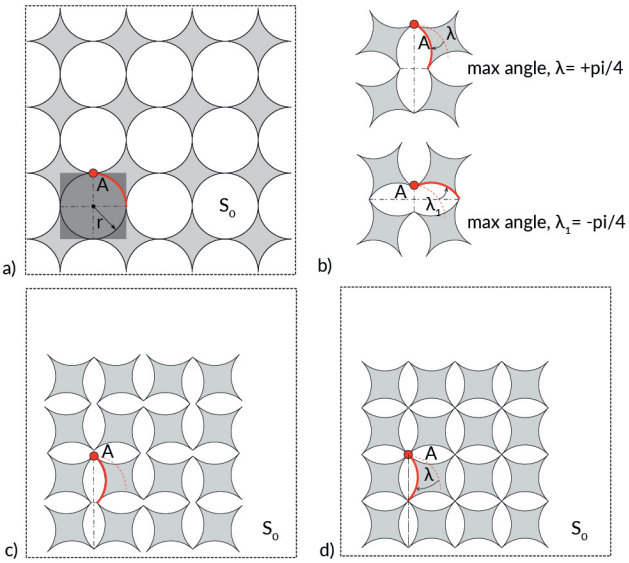

6

6 a) Profile curve is a circular arc with radius r, b) two different rotation directions, c) one of the activation positions, d) maximum rotation and minimum porosity in the kinematic system.

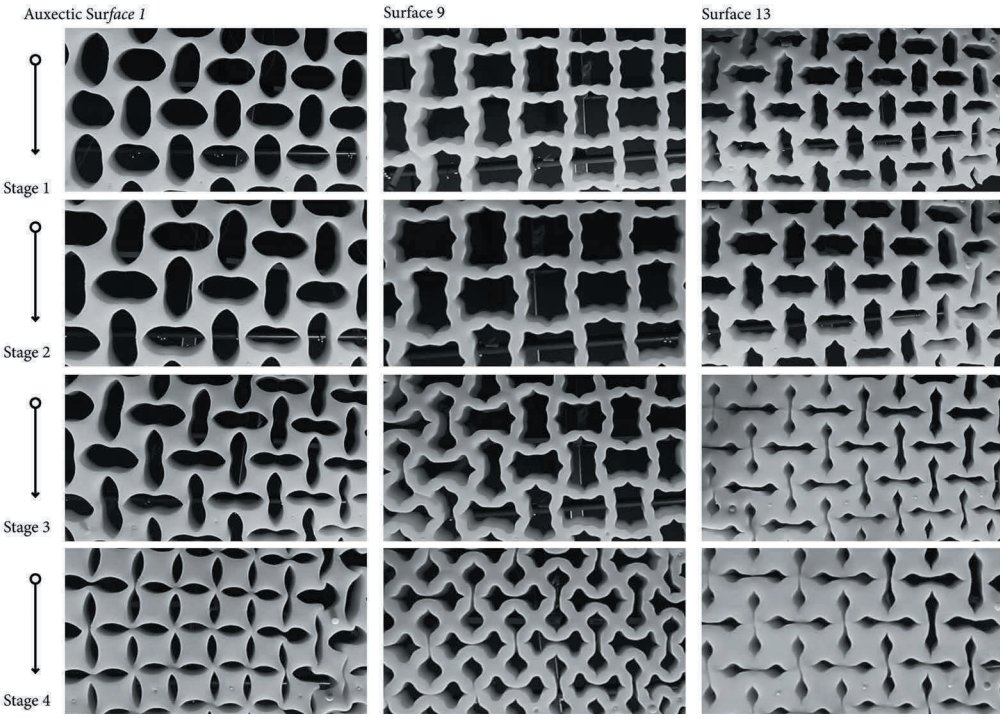

9

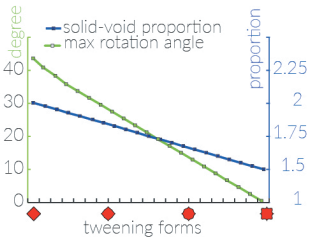

7

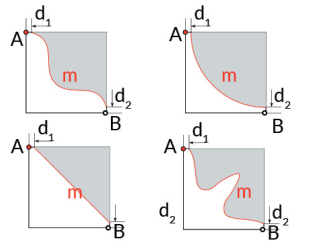

8

7 Shows the relation between four different m curves, their corresponding perforations, their resulting angles, and thus degrees of porosity.

Changes of the Boundary Area of the Kinematic System

As the kinematic system undergoes various stages, its original boundary area S0 also changes (Figure 5). The relation between solid and void in the three different positions are 1:1 (Figure 5a), 1:0.5 (Figure 5c) and 1:0 (i.e., without voids when it reaches its maximum activation). Furthermore, the auxetic material moves in relation to the activation point A. By choosing a different activation point, the overall system size will scale in relation to that point. Summarizing, the area of the void for profile curve m as a diagonal line can be calculated as: Area (void)= 4m(length)*sin (max angle−λ)2*cos (max angle−λ)2. Figure 6 shows an arc as the profile curve m and an activation point A. Figure 6b shows two possible rotations: clockwise and counterclockwise. Figure 6c shows a stage rotating clockwise around point A and Figure 6d shows the maximum position where the points of the arcs encounter. In the rotation, the ratio of areas between solid and void is pi:2. The void area is calculated as: Area (void)= (r2 pi) − 4 *sin (max angle−λ)2*cos (max angle−λ)2.

We conclude that for a planar periodic pattern, the geometrical and mathematical behavior of auxetic systems is based on one-parameter deformations. One-parameter deformation is defined by the angle λ that directly influences the movement of the auxetic system. If the angle is pi/4 and the profile curve is a diagonal line, the whole system can close with zero porosity. The angle resulting from the tangent of different profile curves would generate different porosities (Figure 7). In the following section the impact of materiality on these principles will be investigated.

Geometric Principles: Response to Materiality

The above analysis did not assume a material thickness at the hinges and did not consider the elastic material deformation. When intending to design an auxetic system for physical prototyping, altering the geometry around points A and B, and including a material offset (hinge) d1 and d2 was necessary (Figure 8). The hinge's width is related to the particular material onto which the initial perforations are created, and relates to the expected tolerance and scale of the fabrication process. The hinge thickness determines the overall stiffness and geometric response of the auxetic systems. The relation of hinge width and length determine its slenderness—a key factor that impacts buckling. Early physical prototypes were produced from cast rubber using a range of periodical patterns (Figure 9).

The deformations observed on physical prototypes were confirmed using non-linear FEA using Abaqus version 6.12 (Figure 10). The pattern was loaded uniaxially from the top while keeping the bottom support fixed using the following parameters: Young's Modulus, E = 1.0e6 N/m^2, Poisson's Ratio nu = 0.499, Density = 1150.0 kg/m^3.

8 Position of profile curve m in the "material world."

9 Physical prototypes showing buckling and different stages of activation.

10 Hinge details showing FEA simulation of periodical pattern and degrees of buckling. The deformed shape correlates closely with the observation of the prototypes.

The computational geometric study of auxetic surfaces revealed a set of geometric rules highlighting the importance of the cell geometry on the overall deformation behavior. Once integrating materiality and thickness in the geometric model, the system can be modeled as an overall elastic solid such that non-linear finite element methods well-approximate the deformation behavior. Based on the understanding of geometry and materiality, a parametric model was developed to facilitate the design of various patterns. The parametric model did not attempt to represent buckling and material deformations as observed during the FEA studies. Instead, the focus was on rapidly producing patterns that are known to exhibit buckling and lead to the desired overall surface transformations. The parametric model allows the user to modify the profile of curve m, the number and proportion of quadrants, the width of hinges, and the angle and direction of actuation. The model was used to generate pattern designs that were prototyped at various scales. A new digital workflow was created that allowed for seamless data export to Abaqus for FEA studies, further accelerating design iterations and prototyping.

Having a computationally integrated way to understand different cell geometries in auxetic surfaces enables designers to engage both physical and computational realms in the design process. This workflow allows for a rapid comparison of results. The following section expands the vocabulary of pattern design to non-standard situations that involve variations not previously researched by others.

PATTERN VARIATIONS

The emergence of robust digital workflows and the availability of CNC and robotic fabrication technologies has triggered a broad interest into non-standard geometries of architectural components. Can auxetic surfaces be designed for non-standard situations, and include variable degrees of porosity (understood as the varying ratio between solid and void) within the same material, while maintaining controlled contraction and expansion behavior? This section discusses the repercussions of changing the scale of perforations and spacings while maintaining the same parametric profile curve m, as well as tweening cell geometries that involve the mathematical blending of different profile curves across a patterned surface. These operations open up new territories for auxetic designs and allow for the accommodation of surface patches with non-orthogonal edges that, in an architectural context, would provide much needed design flexibility for adapting surface tessellations to irregular surface geometries.

10

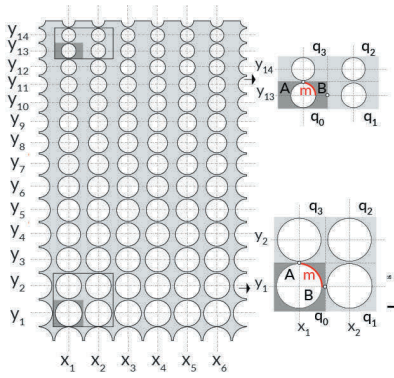

11

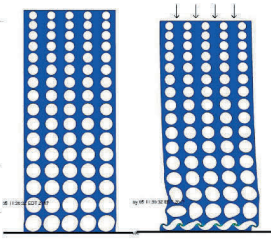

12

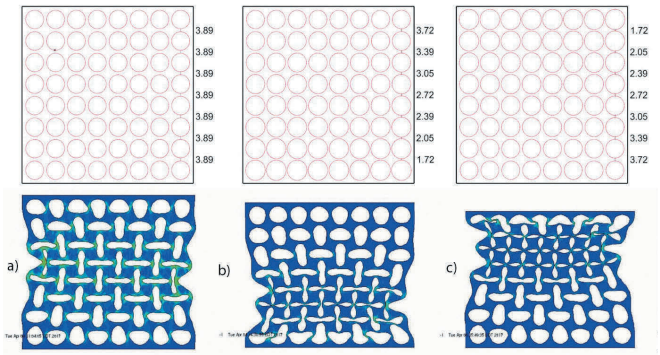

13

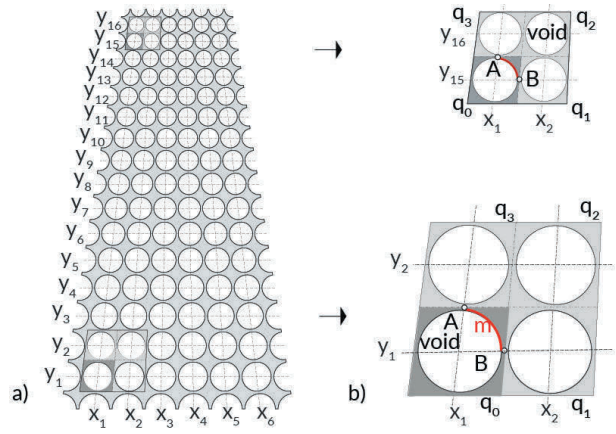

14

11 a) Pattern showing scale transformation from Y1 to Y14, b) quadrant detail on Y13Y14–X1X2 above and quadrant detail on Y1Y2–X1X2 below.

12 FEA simulation showing scalar transformation from Y1 to Y16, initial and actuated stages

13 FEA simulation studying the effect of varying hinge slenderness for uniform cell shapes: a) hinges are equal throughout, b) hinge slenderness increases from top to bottom, c) hinge slenderness decreases from bottom to top.

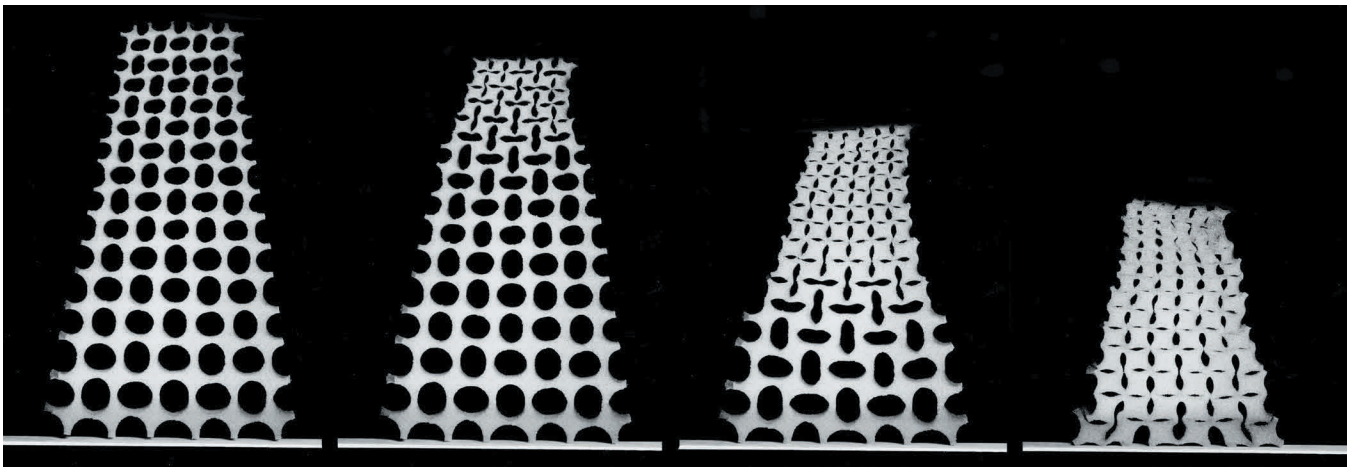

15

Scaling

The effect of scaling was first investigated by analyzing the changes that result when same-shaped perforations are scaled while maintaining their y-direction spacing in the orthogonal grid (Figure 11). In this operation, the shape of the perforations was kept constant and the ratio between solid to void in the x axis increased as the size of perforations decreased. In the FEA simulations a uniaxial compression was applied at the top of the pattern, which was rigidly fixed at the bottom (Figure 12). Both local cell buckling, subsequent rotation, and overall buckling of the patterned sheet was observed. Local buckling occurred when the slenderness of the hinge was such that buckling and rotation preceded the simple compression of the material. The overall behavior confirms the fundamental principles of ratio solid/void laid out by the Bertoldi group, but shows that these principles also apply when the size of the opening changes in a single auxetic surface. A second set of studies was conducted, now positioning zones of greater hinge slenderness (smaller hinge width compared to their length) in the lower zone of the sample (Figure 13b) or the upper zone (Figure 13c). The buckling behavior was compared with a control sample featuring uniform hinge slenderness throughout (Figure 13a). The study demonstrates that buckling first occurs in zones of greatest hinge slenderness, with minor differences in slenderness being sufficient to either produce or defray buckling-type deformations.

Subsequent set of studies included skewing the initial grid such that the spacing between perforations was proportionally maintained as the size of perforations decreased proportionally. Figure 14 shows that the shape of the perforations and their orientation within each row remained constant. The simulations showed uniform buckling behavior throughout the whole auxetic surface (Figure 16). Deformation irregularities at the top and the bottom of each sample reflect the existence of specific constraints near the support region and the loading zone. Figure

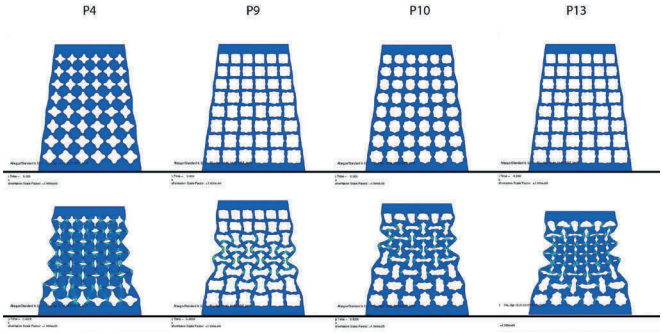

16

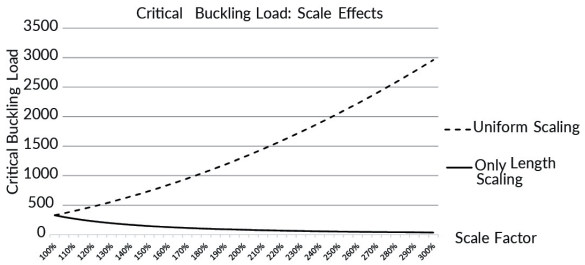

17

14 a) Pattern showing scale transformation from X1 to X6, and Y1 to Y16 , b) quadrant detail on Y15Y16–X1X2 above and quadrant detail on Y1Y2–X1X2 below.

15 FEA simulations showing some of different scaling with different shape perforations. Top row denotes initial uncompressed stages and bottom row shows compressed stages.

16 Physical prototype showing scale transformation from Figure 14.

17 Scale effects for a column with fixed supports.

18 Tween between different profile curves m on a square boundary.

19 FEA simulation of pattern generated by tweening between different perforations and different stages of actuation. Top row denotes initial uncompressed stages and bottom row shows compressed stages.

20 Physical prototypes and different stages of actuation. The picture on the left shows the initial uncompressed stage. The center and right pictures show stages when the surface is compressed.

21 Pattern generated by tweening between different profile curves m. The perforations interpolate proportionally.

15 shows a physical prototype confirming the results of the FEA study, in this case using circular cell profiles.

The physical prototype allowed for the observation of time effects. Upon imparting a displacement at the upper edge, the sample first showed buckling-related deformation at the top, which increasingly spread towards the bottom area with its larger-scale cell features. The slender hinges at the top are more compliant, and therefore exhibit buckling before the stiffer hinges at the bottom (Figure 15). The behavior confirms the validity of the Euler equations that generally govern buckling, whereby the critical buckling load P equals $\pi EI/L^2$. Figure 17 shows the effects of scaling length and moment of inertia of a column with fixed supports, a system analogous to a single hinge strut in the auxetic systems subject to this study. The dashed curve represents the effect of uniformly scaling both length and moment of inertia, whereas the continuous line curve represents the effect of scaling only the length of the column. The critical buckling load increases quickly as both length and the moment of inertia of the column scale equally—confirming why the sample of Figure 16 buckles first when cell size and hinge width are small.

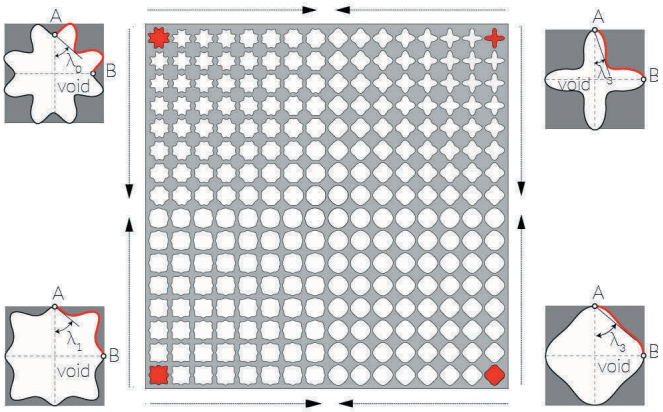

18

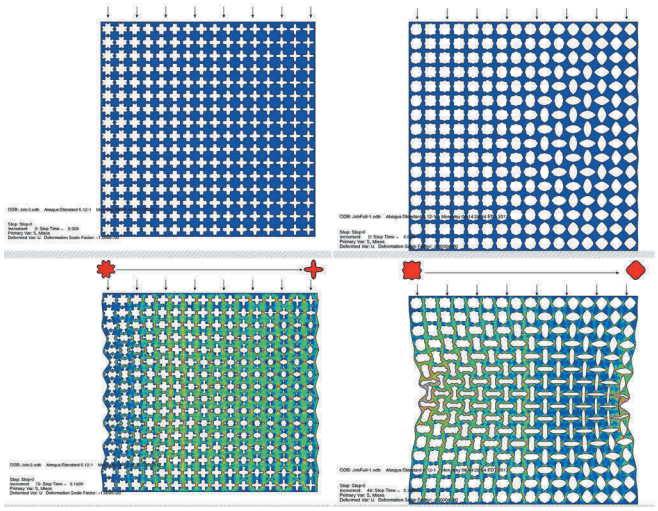

19

Tweening

A different set of samples was created through tweening between different-shaped perforations, understood as the intermediate geometric frames between two distinct geometries. Figure 18 shows four different perforations (in red) at the corners of a square auxetic surface. The rest of the perforations within that surface were generated by tweening fourteen frames in between

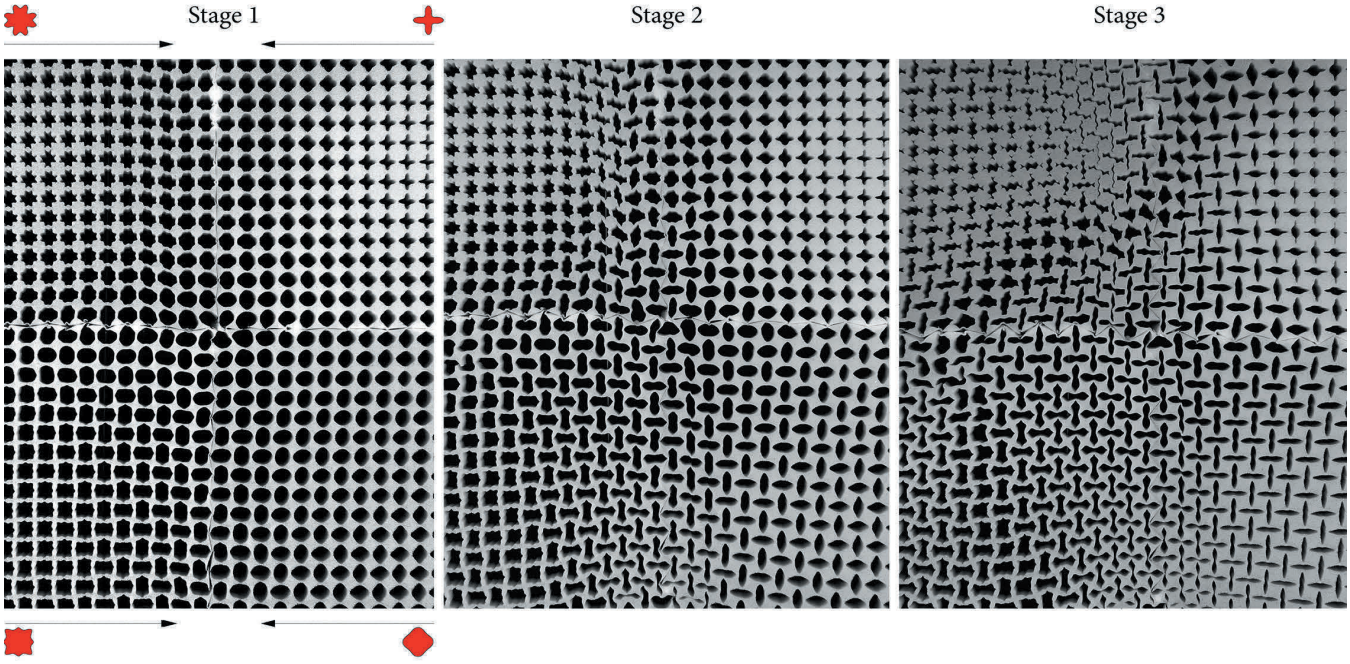

20

the initial perforations both vertically and horizontally. The remaining perforations were created by tweening between the newly generated top and bottom perforations. The undeformed surface shows different profile curves m, which show different angles λ of rotation and different degrees of porosity when actuated. When actuated, the effect is an overall gradient of porosities within the same auxetic surface, evident both in the FEA simulation (Figure 19) and in the physical prototypes (Figure 20).

Combined Scaling and Tweening

Finally, samples that featured a combination of pattern scaling and tweening (Figure 21) were studied through a combination of geometrical modeling, the corresponding FEA, and physical prototypes. The main parameter for determining a buckling-based deformation is the relation between length and moment of inertia of the hinge thickness. Designers have the freedom to choose different profile curves m (and thus perforation shapes) as long as the length-to-stiffness ratio of the surface hinges remains small enough to have buckling precede

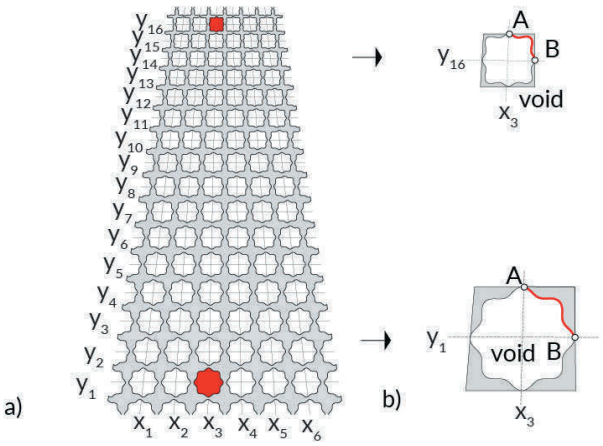

21

unidirectional compression. Both FEA and physical prototypes confirm that behavior (Figure 22). These different pattern studies equip the designer with a range of possibilities for controlling the degree of porosity within a single auxetic surface. The next section applies the underlying rules to a design experiment at the architectural scale.

PROTOTYPING AT ARCHITECTURAL SCALE

Digital Fabrication Strategies

Earlier work by Bertoldi (Babaee et al. 2013) had relied on producing molds to cast elastomeric polymers as samples that allowed the study of buckling patterns in auxetics. Casting, however, proved cumbersome and difficult for surface with sizes in the meter range. 3D printing of auxetic surfaces, while potentially interesting, presented scale barriers, but printing remained an excellent technique for understanding pattern behavior on a small scale, and studying the effects of using multiple materials in a single auxetic surface. Instead, laser cutting and robotic waterjet cutting techniques were tested and developed to facilitate an integrated digital workflow from the parametric model, and accelerate the design-to-prototype schedule. These digital fabrication tools, once integrated with the parametric geometry model, allowed for non-standard patterns to be efficiently produced. They also allowed the fabrication of pieces at architectural scales. A waterjet attached to a 6-axis robotic arm allowed for fast prototyping and production of larger-scale prototypes while maintaining the required accuracy for the intended performance. Code was generated using MasterCam/Version X7. A series of test cuts established the best cutting speed in relation to the type of elastic material used. Best results were achieved by cutting only with water, without the abrasive additive. Accurate perforations of silicone slabs ¼″ to 4″ thick were achieved with water pressure of 600 psi (Figure 23). Starting at

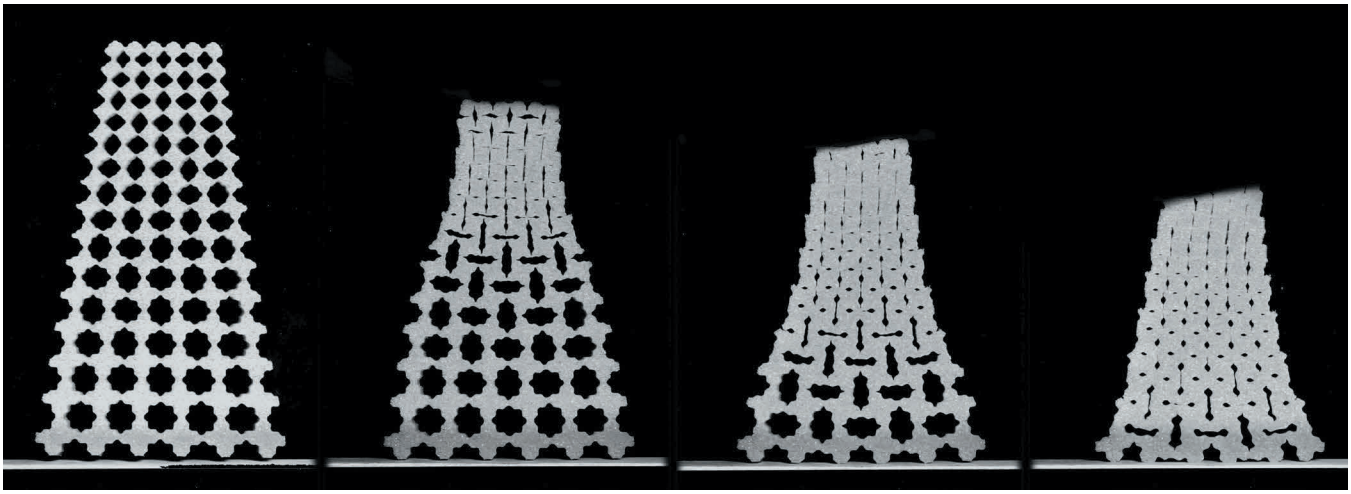

22 Physical prototype of pattern generated by tweening techniques.

22

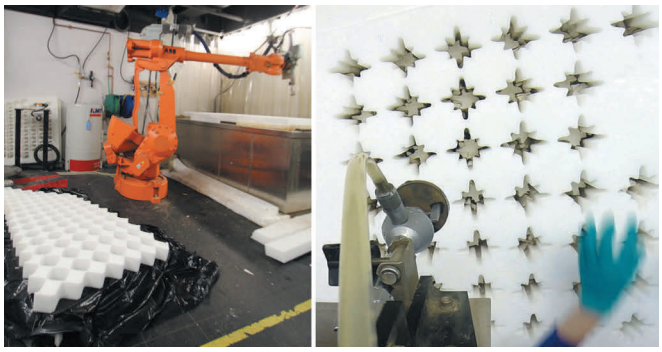

23

23 Waterjet attached to a robotic arm; patterns cut from polyurethane foam using waterjet.

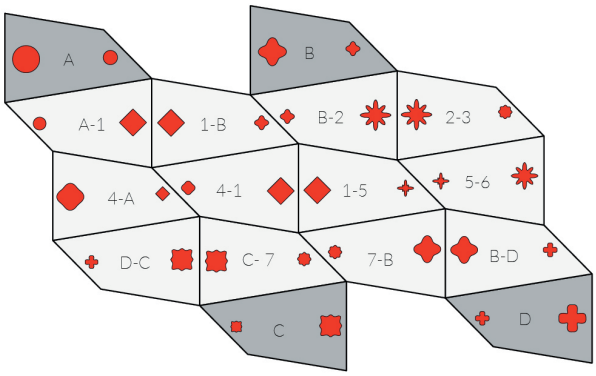

24

24 Organization of auxetic surface modules as scaling types: A, B, C, and D and tweening/scaling subtypes: A-1, 1-B, B-2, 2-3, 4-A, 4-1, 1-5, 5-6, D-C, C-7, 7-B, B-D.

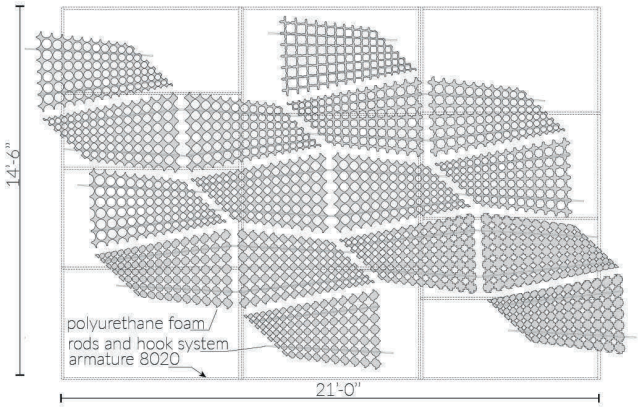

25

25 Plan for sixteen auxetic surfaces.

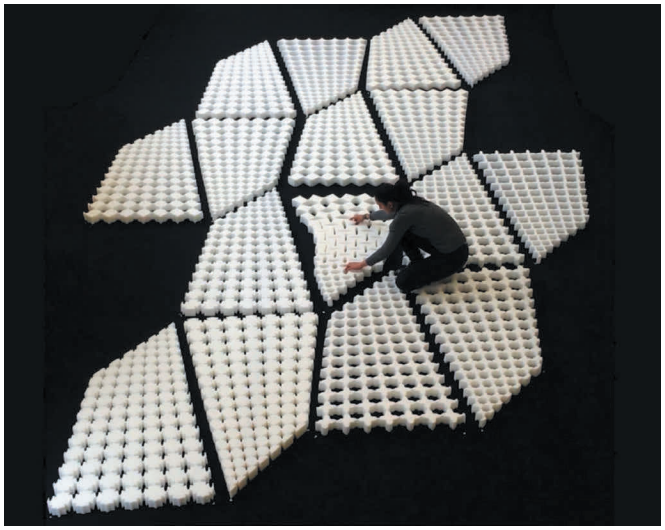

26

26 Modules, just prior to installation.

the perforation's center with a lead-in cut, and working towards the perimeter ensured an accurate cut necessary to achieve the intended thickness for the material "hinges" with a precision of 0.01 mm to achieve buckling behavior.

Case Study

An architectural installation was designed and built (Figure 1) to test the applications of design principles governing auxetic surfaces. The designed structure is comprised of sixteen auxetic surface modules. Surfaces were defined as types A, B, C, D and subtypes based on their performative qualities (Figure 24). The overall pattern was distributed across all modules requiring careful calibration to ensure proper buckling behavior and hinging behavior throughout (Figure 25). Each module displays different degrees of porosity, contracting and expanding in a controlled manner when actuated through an external mechanism. The overall result is a constantly changing structure that filters light in response to the occupant's input. A main consideration was to design a range of patterns that would generate attractive configurations and light effects in both their compressed and their expanded stages (Figures 27b and 27c). Fabrication involved cutting perforations from 4′ x 8′′ x 3′′ polyurethane foam sheets using the 6-axis robotic waterjet. Each surface contains around 128 perforations ranging from 30–90 mm cell size, leaving hinges ranging from 2–5 mm width. Fabrication took less than 30 minutes per surface, compared to 6 hours when cutting the same designs using a laser cutter. The auxetic modules were suspended from a rods and hook system, permitting them to slide along supporting rails during actuation (Figure 27a). Actuation was achieved through a system of single-piston struts that displaced four points of the auxetic surface by means of hinging extensions. Piston displacement and length of the extensions were calibrated to match the displacement in the parametric model, validated by FEA studies. A user-friendly tablet interface that permitted occupants to control a desired porosity setting in real time (Figure 27d).

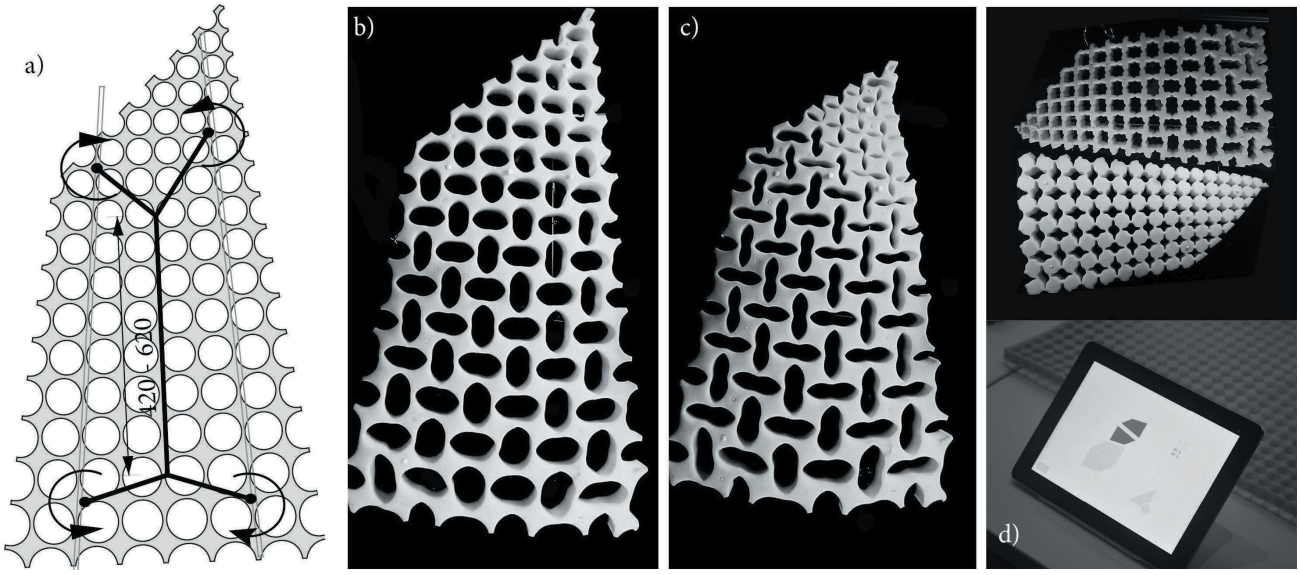

27

27 a) A single piston was designed to actuate the entire surface through hinging extension struts, b) surface before actuation, c) actuated surface, d) occupants were able to control the movement through a table interface.

CONCLUSION AND FUTURE WORK

Auxetic metamaterials can be parametrically modeled with sufficient accuracy to allow for the design of systems at architectural scale. New contributions on scaling and tweening of auxetics expand the design scope of systems that promise to challenge the current paradigm of kinetic mechanisms for adaptive architectural elements where varying porosity is desired. The case study tested principles of auxetic surfaces that can be further applied to other architectural components, such as facades, screens, or shading systems. By creating integrated digital workflows of geometrical modeling, FEA, and digital production systems, a rapid exploration of conceptual design to prototypes is efficiently linked. Non-Linear Matter: Auxetic Surfaces presents an integrated material system that delivers high-capacity transformation with minimal hardware needs. Further research is needed to understand the practical limitations of material fatigue on the hinges and explore possible structural and acoustical applications. Robotic technology brings about additional opportunities that further expand the understanding of two-dimensional auxetics into a third dimension by permitting angled cuts and asymmetric hinge rotation. Use of topographical, textural, and color changes on the solid portions could provide visually compelling yet technically simple design expansions of adaptive material systems based on auxetics. Regarding actuation, gel-based actuation systems that respond to moisture content show early promise, but require further refinement and development in order to achieve the robustness needed in building applications. The research constitutes a promising step towards the design of responsive structures, where on-demand changes of surface porosity are advantageous in scenarios such as lighting control, air flow. or acoustic manipulation.

ACKNOWLEDGEMENTS

Thanks to Katia Bertoldi and Johannes Overvelde from the Harvard John A. Paulson School of Engineering and Applied Sciences for their contributions and FEA consulting, to Panagiotis Michalatos and Malika Singh from the Harvard MaP+S Group, Onye Ahanotu, Jack Alvarenga from the Wyss Institute for Biologically Inspired Engineering for their contributions to research and design. Thanks to Anu Akkineni, Palak Gadodia, Kevin Hinz, Apoor Kaunik, James Weaver and Jane Zang for helping with the construction of the final installation.

REFERENCES

Álvarez Elipe, Juan Carlos, and Andrés Díaz Lantada. 2012. "Comparative Study of Auxetic Geometries by Means of Computer-Aided Design and Engineering." *Smart Materials and Structures* 21: 105004.

Babaee, Sahab, Jongmin Shim, James C. Weaver, Elizabeth R. Chen, Nikita Patel, and Katia Bertoldi. 2013. "3D Soft Metamaterials with Negative Poisson's Ratio." *Advanced Materials* 25 (36): 5044–49.

Bertoldi, K., M. C. Boyce, S. Deschanel, S. M. Prange, and T. Mullin. 2008. "Mechanics of Deformation-Triggered Pattern Transformations and Superelastic Behavior in Periodic Elastomeric Structures." *Journal of the Mechanics and Physics of Solids* 56 (8): 2642–68.

Evans Kenneth E., and A. Alderson. 2000. "Auxetic Materials, Functional

Materials and Structure From Lateral Thinking." *Advanced Materials* 12 (9): 617–28.

Greaves, G. N., A. L. Greer, R. S. Lakes, and T. Rouxel. 2011. "Poisson's Ratio and Modern Materials." *Nature Materials* 10 (11): 823–37.

Ivens, Jan, Matheiu Urbanus, and Carl De Smet. 2010. "Shape Recovery of Thermoset Shape Memory Polymers and Fibre Reinforced Shape Memory Polymers." In *Proceedings of the 14th European Conference on Composite Materials*, 005:1–005:10. Budapest, Hungary: ECCM.

Jacobs, S., C. Coconnier, D. DiMaio, F. Scarpa, M. Toso, and J. Martinez. 2012. "Deployable Auxetic Shape Memory Alloy Cellular Antenna Demonstrator: Design, Manufacturing and Modal Testing." *Smart Materials and Structures* 21 (7): 75013.

Jenett, Benjamin, Sam Calisch, Daniel Cellucci, Nick Cramer, Neil Gershenfeld, Sean Swei, and Kenneth C. Cheung. 2016. "Digital Morphing Wing: Active Wing Shaping Concept Using Composite Lattice-Based Cellular Structures." *Soft Robotics* 4 (1): 33–48.

Körner, Carolin, and Yvonne Liebold-Ribeiro. 2015. "A Systematic Approach to Identify Cellular Auxetic Materials." *Smart Materials and Structures* 24 (2): 25013.

Kshetrimayum, Rakhesh S. 2004. "A Brief Intro to Metamaterials." *IEEE Potentials* 23 (5): 44–46.

Lakes, Roderic. 1987. "Foam Structures with a Negative Poisson's Ratio." *Science* 235 (4792): 1038–40.

Lee, Jae Hwang, Jonathan P. Singer, and Edwin L. Thomas. 2012. "Micro-/nanostructured Mechanical Metamaterials." *Advanced Materials* 24 (36): 4782–4810.

Overvelde, Johannes T. B., S. Shan, and Katia Bertoldi. 2012. "Compaction through Buckling in 2D Periodic, Soft and Porous Structures: Effect of Pore Shape." *Advanced Materials* 24 (17): 2337–42.

Overvelde, Johannes T. B., and Katia Bertoldi. 2014. "Relating Pore Shape to the Non-Linear Response of Periodic Elastomeric Structures." *Journal of the Mechanics and Physics of Solids* 64 (1): 351–66.

Park, Daekwon, J. Lee, and A. Romo. 2015. "Poisson's Ratio Material Distributions." In *Emerging Experience in Past, Present and Future of Digital Architecture, Proceedings of the 20th International Conference of the Association for Computer-Aided Architectural Design Research in Asia*, edited by Y. Ikeda, C.M. Herr, D. Holzer, S. Kaijima, M.J. Kim, and M.A. Schnabel, 725–44. Hong Kong: CAADRIA.

Saxena, Krishna Kumar, Raj Das, and Emilio P. Calius. 2016. "Three Decades of Auxetics Research - Materials with Negative Poisson's Ratio: A Review." *Advanced Engineering Materials* 18 (11): 1847–70.

Walser, Rodger M. 2001. "Electromagnetic Metamaterials." *Proc. SPIE* 4467: 1–15.

Yang, Dian, Lihua Jin, Ramses V. Martinez, Katia Bertoldi, George M. Whitesides, and Zhigang Suo. 2016. "Phase-Transforming and Switchable Metamaterials." *Extreme Mechanics Letters* 6: 1–9.

Yang, Li, Ola Harrysson, Harvey West, and Denis Cormier. 2013. "A Comparison of Bending Properties for Cellular Core Sandwich Panels." *Materials Sciences and Applications* 04 (08): 471-77.

IMAGE CREDITS

All drawings and images by the authors.

Olga Mesa is an Assistant Professor at Roger Williams University and a research associate working with the MaP+S Group at the Harvard Graduate School of Design (GSD). Her primary research lies at the intersection of computer-controlled fabrication and material properties, where she is interested in the accord between form, forces and performance.

Milena Stavric is Assistant Professor at the Graz University of Technology. Her interest lies in architectural geometry and implementation of digital technology and fabrication in architecture and education.

Saurabh Mhatre is a Research Associate in the MaP+S Group at the GSD.He graduated with distinction with a Masters in Design Technology. His interest lies in the synergy between design, technology and materiality.

Jonathan Grinham holds a doctorate at the GSD where his research aims to advance the knowledge of micro-scale materials for thermal regulation in buildings.

Sarah Norman's doctoral work studies self-actuated systems, with particular interest in geometries exhibiting ranges of transformations, explored through additive 3D-printing processes in multiple materials.

Allen Sayegh is an architect, designer, an educator and the principal of INVIVIA. He is an Associate Professor at Harvard GSD and the director of REAL the Responsive Environment and Artifacts Lab at Harvard.

Martin Bechthold is director of the Doctor of Design Program at the GSD, and co-director of the Master in Design Engineering Program at Harvard. He is the founder of GSD's Design Robotics Group and MaP+S Group with its current research focusing on integrating robotic technology into fabrication and construction processes, developing advanced material systems in collaboration with industry partners and the Wyss Institute for Biologically Inspired Engineering.